Eur J Anat, 10 (3): 101-113 (2006)

Anatomical and histological anomalies in chick embryos from hens immunised to chick embryo soluble and foreign antigens

L. Juárez and A. Rodríguez-Burgos

Unidad de Fetoproteínas, Facultad de Biología, Campus Universitario, C-6, Universidad de Córdoba, Córdoba, Spain

SUMMARY

The anatomical and histological alterations that affect chick embryos from hens immunized with antigens from chick embryos, but which are foreign to the immune system of the hen, are reported here for the first time. The importance of these antigens, the maternal antibodies that they induce, and the injuries that these produce in the embryo can clearly be seen in the results reported. These results, obtained by means of experimental immunization in hens, may also hypothetically take place in humans (women) through natural immunization because analogous antigens from the embryo cross her placenta.

Thus 81 eggs of immunized hens were studied, of which 60 displayed morphologic alterations of diverse intensity, especially developmental delay and growth retardation. Of these, three embryos 57 pih, 4 and 7 pid were chosen for their delay in growth, during the period of organogenesis. Their anatomical alterations were studied and an exhaustive and qualitative histological analysis was carried out. Each section was compared with those of control embryos which underwent the same time of incubation or were at the same stage of development. Embryonic growth retardation was evident in the smallest size of the embryos but also there were developmental delay of some organs and cells. Among other striking anomalies, the following were observed: invasion of the neural crest cells into the mesencephalon and rombencephalon lumen; malformation of the *infundibulum*; disintegration of dermatomes and myotomes; a loose arrangement of mesenchymal tissue; a delay in the development of the heart and blood islands cells, etc. Some of the observed anomalies were related to birth defects that also affected other chicks in the same experiment, as published elsewhere.

Key words: Embryonic developmental delay – Mesenchymal anomalies – Neural anomalies – Infundibulum anomalies – Myotome anomalies

Abbreviations: GC: Growth control embryos; Exp: Experimental embryo; DD: developmental delay; GR: Growth retardation; HH: Hamburger and Hamilton, 1951; IC: Incubation control embryos; pid: Post incubation

Submitted: May 5, 2006
Accepted: October 25, 2006

Correspondence to:
Prof. A. Rodríguez-Burgos. Unidad de Fetoproteínas, Facultad de Biología, Campus Universitario, C-6, Universidad de Córdoba, 14071 Córdoba, Spain. Phone and Fax: +34 957 218650. E-mail: a.r.burgos@uco.es

day; pih: Post incubation hour; sAlloAg: Soluble alloantigens; sF-TrAg: Soluble foreign transitory antigens; sFF-Ag: Soluble foreign foetal antigens (sF-TrAg and sAlloAg).

Introduction

Since 1950 there has been increasing interest in the alterations that take place in chick embryos when they were inoculated with heteroantibodies against antigens of chick embryo extract (Mun, 1958) or the adult chicken, obtained for example from the lens (Clarke and Fowler, 1961; Langman et al., 1962; Genís-Gálvez et al., 1967) or the brain (McCallion, 1971), or only differentiation antigens, such as alpha-fetoprotein, obtained from chick embryo blood (Smith, 1973; Sánchez Palazón et al., 1996) (see more references in Rodríguez-Burgos, 2003). These heteroantibodies were obtained from rodents that of course produced antibodies against all the proteins of chick embryo extracts and of adult chickens without discrimination, since all of them were foreign antigens for the rodents. The consequences were monstrous embryos, foetal death and a size reduction of the chick embryos. When an antiserum against a purified protein was obtained and their IgG were later purified to administer them into chick embryos (Langman et al., 1962) or chick organ cultures (Sánchez Palazón et al., 1996) or when the antiserum was absorbed with antigens from other adult organs and their IgG were purified (McCallion, 1971), the results were more specific and limited to certain tissues.

This method underwent a Copernican change when chick embryos were given isologous antibodies coming from their dams (hen), because these underwent an experimental active immunisation with the antigens from the chick embryo extract (Rodríguez-Burgos, 2003), which mimics what happens naturally in women, when they are immunised with the antigens from their embryos and the antibodies induced in them are transferred to their offspring, e.g. Rh antigen. Indeed, antigens from the embryo extract that also exist in the dam are «self» for her and, therefore, do not induce antibodies in her; on the contrary, the dam produces antibodies against the antigens of the extract that are "non self" or foreign for her. In the present work, we used nine chick embryo soluble and foreign antigens (sFF-Ag), of which five were soluble, foreign and transitory antigens (sF-TrAg) and four were soluble alloantigens (sAlloAg).

Once the existence of this class of fetoproteins (sF-TrAg) was known, that sAllAg had not been studied in embryology, and that the embryos born of hens immunised with all of them (sFF-Ag) displayed diverse alterations in gross anatomy and especially developmental delay and growth retardation in their offspring, we decided on the one hand to analyse the macroscopic alterations, developmental delay and growth retardation, of the assembly of the collected embryos (Rodríguez-Burgos and Juárez, unpublished observations) and, on the other, to perform the present study: an exhaustive and qualitative account of the alterations in the gross anatomy and histology, induced by anti sFF-Ag isoantibodies, in three chick embryos at different stages: from the start of organogenesis to approximately the end of this period. We also discuss the anatomical and tissue structures that did not show any alterations. Finally, we explore the possible relationships between some of the anomalies described here and the congenital anomalies displayed by chicks born alive in the same experiment (Rodríguez-Burgos, 2003), which have been described in detail elsewhere (Rodríguez-Burgos et al., unpublished observations).

Materials and Methods

The preparation of the chick embryo extracts has already been described, with embryos that had been incubated for 53 h, the sequence of immunisation of the hens, the inoculation of the control hens, the incubation of the immunised hens' eggs and the control hens, and the detection of the sFF-Ag by Western immunoblot, etc. (Rodriguez-Burgos, 2003).

1. ANATOMICAL STUDY AND DETERMINATION OF GROWTH

Experimental embryos (Exp) were chosen from a total of 60 abnormal embryos. Among these, developmental delay (DD) and growth retardation (GR) was the most constant disorders. We used three chick embryos undergoing DD and GR at different stages, from the start of organogenesis to approximately the end of this period. In order to detect these disorders we

used, depending on the case, a magnifying glass or a microscope. These three Exp, which had been incubated for 57 pih (post incubation hour), 4 pid (post incubation day) and 7 pid, were compared with control incubation embryos (IC) in order to determine the intensity of the DD and GR. IC were obtained from eggs from the control hens that had been inoculated with PBS, Freund's adjuvant and a protective cocktail. Once all the data from the comparative gross anatomical study of each Exp with their corresponding IC had been collected, we would be able to know at what stage of development and growth it was, according to HH (Hamburger and Hamilton, 1951). We then obtained a growth control embryo (GC) for each Exp: a chick embryo at the same stage of development and growth as the Exp (but from a hen that had not been treated with any compound) in order to visualize the existing histological anomalies. Thus, we obtained two kinds of controls for the Exp: **IC:** with the same ***incubation time*** as each Exp, and **GC:** with the same ***degree of development and growth*** as each Exp.

2. PROCESSING OF SAMPLES FOR OPTICAL MICROSCOPY

We followed standard methods (García del Moral, 1955). However, some significant details are reported:

Preparation of sections: After the process of infiltration, we decided to divide each embryo into cutting areas. Then, the whole piece and the aforementioned cutting areas were measured with a micrometer. The specimens measured between 2,500 μm (the smallest) and 11,500 μm (the largest). Each section was 2.5 microns thick and each serial section was made up of nine sections (always cross-sectional to the cephalic-caudal axis). Three were dyed with haematoxylin-eosin and the others were kept as reserves. The measurement, in microns, of each cutting area of the specimen determined the number of serial sections to be made, and how much of the piece we would have to trim between serial sections. In areas that contained a larger number of tissues with more complex structures, more serial sections were cut. For each specimen, an average of 45 serial sections were cut, regardless of its overall size, and they were distributed as indicated in Results. *Embedding*: The samples were infiltrated at room temperature with a solution made of Hydroxyethyl methacrylate (50 ml) and Benzoyl peroxide (0.1 g). The infiltration process was carried out using two 15-minute baths. Next, the samples were placed in embedding solution (at room temperature) made of the infiltration solution (15 ml) and dimethyl sulfoxide (catalyst) (1 ml). *Staining*: All samples were dyed with modified Harris' haematoxylin and Eosin Y (C.I. Nº 45380). *Photographs*: These were taken with a Kodak DC 120 digital camera connected to an Olympus SZX9 magnifying glass, and those of the histological sections were taken with a digital Nikon Coolpix 4500 connected to a Zeiss Axiostar microscope. *Morphometric analysis*: In some areas we applied morphometric measurement for the sake of interest. The software used was Image Pro-Plus, version 2002 (Media-Cybernetics Company). The microscope used was a Nikon Eclipse-400, calibrated using its own software. Finally, the images were obtained with a RGB 3 DCC camera, JAI, model 1490.

RESULTS

1a. COMPARATIVE ANATOMICAL STUDY OF THE 57 PIH **EXP** (11 HH) AND ITS 57 PIH **IC** (16 HH)

The results are summarised in Table 1.

Comments: The length was measured from the neuropore to where the primitive streak disappeared. The formation of extra-embryon-

Table 1: Developmental stage of the Exp-57 pih and its control embryos. Anatomical differences between the Exp-57 and its incubation control embryo, which had the same incubation time.

EMBRYO	EXPERIMENTAL	INCUBATION CONTROL	GROWTH CONTROL
Post incubation hours	57	57	43
Stage according to pih	16-17 HH	16-17 HH	11 HH
Stage according to its growth	11 HH	16 HH	11 HH

ANATOMY	EXPERIMENTAL	INCUBATION CONTROL
Length of embryo	4.8 mm	9.0 mm
The somites	13 pairs (HH stage 11)	27 pairs (HH stage 16)
The amniotic fold	A small crease is beginning to protrude	Extended to the 11th pairs of somites
The limb buds	Not visible	Not visible
Torsion	Not begun	Head twisted round to the right

ANATOMY	EXPERIMENTAL	INCUBATION CONTROL
The primitive streak	Present (0.4 mm in length)	Not present
The tail bud	Not visible	A short cone
The pineal gland	Not visible	A slight promontory
The nervous system	Three cerebral vesicles (40-45 pih): prosencephalon, mesencephalon, rhombencephalon. 11 neuromeres	Telencephalon (57 pih), diencephalon, isthmus, mesencephalon, metencephalon, myelencephalon
Rathke's pocket	Not visible	Visible
The neural groove	Open	Closed
The auditory vesicle	Not visible	Visible
The unsegmented mesoderm	1.3 mm	1.0 mm
The vascular system:		
- The omphalo-mesenteric arteries	Not visible	Both are visible at the level of the 18th pair of somites surpassed
- The vitelline veins	Visible	They are present but not visible due to fold of the *area pellucida* and the looping of the heart
The heart:		
- Lateral development (dorsal view)	The primordia are bent to the left instead of towards the right. Special delay of the growth	
- Approximate age (according to development) and HH stage	29-32 pih and HH 9	54-60 pih and HH 16
- Position	At the same level as rhombencephalon	At end of myelencephalon
- Looping process	Hardly begun	Fairly advanced
- The aortic arches	Still absent	Three visible complete arches
The ear	Development has not begun. Auditory placodes are not visible. Ear development is inferior to 35 pih	Auditory vesicle and endoplasmic duct are visible
The eye	Primary vesicles. Eye developmental delay is greater than that of a 40 pih embryo	Optic cups, choroid fissure and lens
The gut:		
- Length	1.5 mm	3.0 mm
- Position of the anterior intestinal portal	1st – 2nd somites	16th somites
- The pharyngeal pouches	Not visible	Three pouches are visible
- *Stomodaeum*	Not visible	Visible
- The posterior intestine	Not visible	Visible
Bending	No bends	Three normal bends
The *area vasculosa*	Mottled appearance. Blood islands 26-29 phi and HH 8	Vessels
The branchial grooves	Not yet appeared	First three are visible
The tail bud	Not yet appeared	Visible, like a short cone

ic blood vessels showed greater signs of delay than the rest of the embryo, because, given the number of somites (13), this embryo corresponded to stage 11 HH (40-45 pih), whereas the development of blood islands placed it at stage 8 HH (26-29 pih), with four pairs of somites. The development of the heart showed greater signs of delay than the rest of the body, since the development of the heart placed it at stage 9 HH (29-32 pih), with seven pairs of somites (Bellairs and Osmond, 2005).

1b. COMPARATIVE HISTOLOGICAL STUDY OF THE 57 PIH **EXP** (11 HH) AND ITS 43 PIH **GC** (11 HH)

Cutting Area A (10 serial sections)**. - The Head Ectoderm. Exp:** The cells were flat in the dorsal part of the prosencephalon, then becoming rectangular when they advanced towards the lateral and the ventral part of the prosencephalon. The nuclei stained well and the cytoplasm was hyaline. Cracks were seen (Figure 1). **GC**: the cells stained well. No cracks were seen (Figure 2). **The Prosencephalon. Exp:** the prosencephalon became ovoid in shape, with an axis set transversely through the centre and optic vesicles at the ends. Their extended cells had radials to the lumen and were in columns of three to four elements. The cytoplasm was slightly greyish and the nucleoplasm stained well. The cells of the floor showed transparent vacuoles in the area furthest from the lumen. Cracks in the first sections were seen, which later disappeared. As we moved further along the sections

we noticed a tendency towards cellular disintegration. In the ventral part there was an accumulation of cells and the orifice that opened there was the *infundibulum* (Figure 1), which assumed an anomalous structure as soon as it ceased to be a depression in the floor of the prosencephalon. **GC:** it was seen that the area of the *infundibulum* was much more developed, flanked by secondary optic vesicles (Figure 2).

Cutting Area B (10 serial sections). **- The Ectoderm. Exp:** In this entire segment the ectoderm displayed wide and clearly visible undulations. The ectoderm that surrounded the dorsal part of the mesencephalon was thinner than in the GC; it was made up of a single cellular layer, but from section B-9 onwards it was made up of two or three layers. It was not hyaline, but did stain well. **GC**: a continuous layer of the ectoderm, whose cells had a hyaline cytoplasm, surrounded the upper half of the mesencephalon. It had fewer but wider undulations. **The Mesenchymal Tissue. Exp:** this displayed a loose arrangement in comparison with the GC.

Morphometric analysis of the area of mesenchymal cells. Although the different concentration of mesenchymal cells in the sections was evident in both the mesencephalon and the rhombencephalon, we wished to place it in objective terms and to quantify it by measuring the area occupied by the aforementioned cells. The values corresponding to the average percentage of the area occupied by the mesenchymal cells in the Exp and the GC are shown (Table 2). The differences are striking.

Table 2. Morphometric analysis of the area of mesenchymal cells in both the mesencephalon and the rhombencephalon from the Exp-57 and its growth control embryo, which had the same developmental stage.

	TISSUE SECTIONS	CELLULAR AREA (%)	INTERCELLULAR SPACE AREA (%)
Exp embryo	1	32,99	67,003
	2	53,49	46,504
	3	47,78	52,21
	Average	**43,875**	**56,116**
GC embryo	1	64,65	35,34
	2	63,19	36,802
	3	55,83	44,16
	4	55,49	44,50
	5	60,12	39,87
	6	67,10	32,89
	7	51,59	48,4
	8	63,27	36,72
	Average	**60,155**	**39,835**

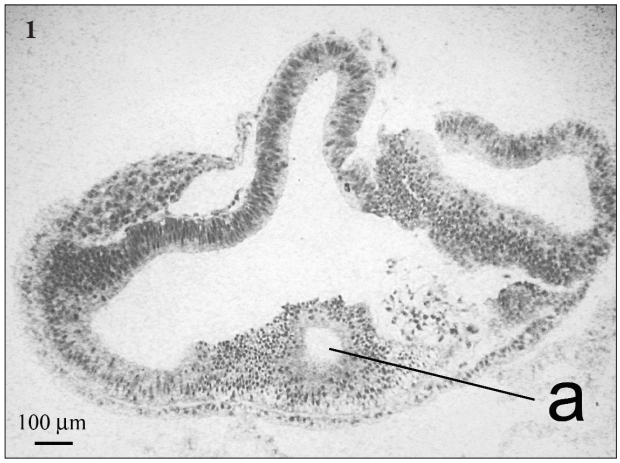

Fig. 1.- Exp-57 pih, H-E (Haematoxylin and eosin). (a) The lumen of the anomalous *infundibulum* is shown.

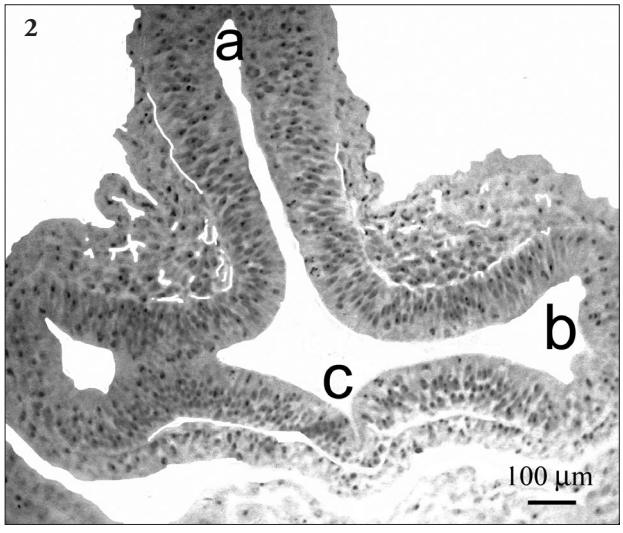

Figure 2. The lumen of the prosencephalon. (b) The lumen of the optic vesicles. (c) The lumen of the normal *infundibulum* is shown.

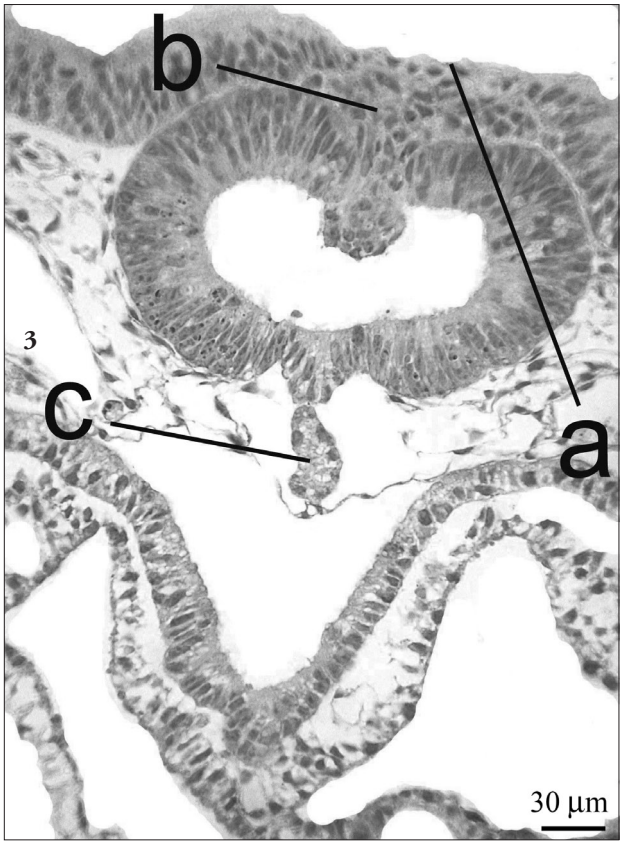

Fig. 3.- Exp-57 pih, H-E. The neural crest cells enter the mesencephalic lumen via the junction that previously joined both edges of the neural tube (a) Ectoderm. (b) Neural crest cells. (c) Notochord.

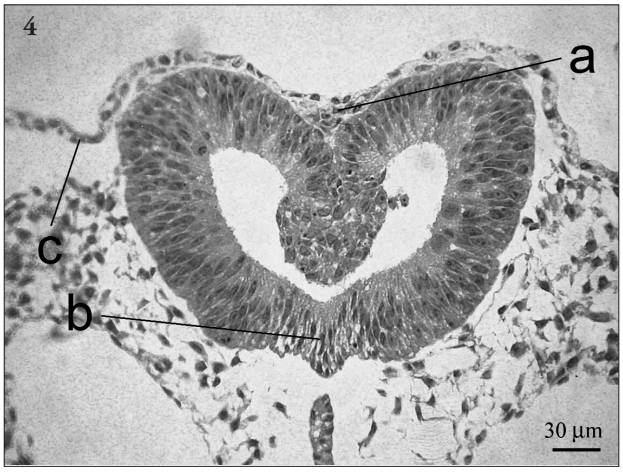

Fig. 4.- Exp-57 pih, H-E. The mesencephalon displays slightly embossed lateral edges. (a) Triangle of neural crest cells. (b) There are clearer cytoplasmatic areas. (c) Ectoderm.

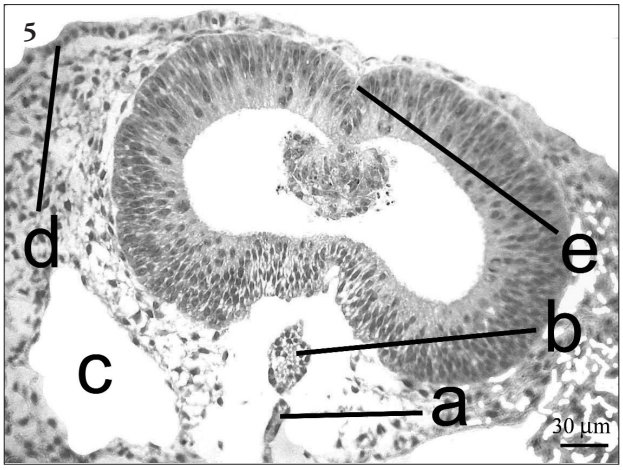

Fig. 5.- Exp-57 pih, H-E. The neural crest cells invade the lumen of mesencephalon. (a) Notochord. (b) Mass of cells released from the mesencephalon. (c) Dorsal aorta. (d) Ectoderm. (e) Neural crest.

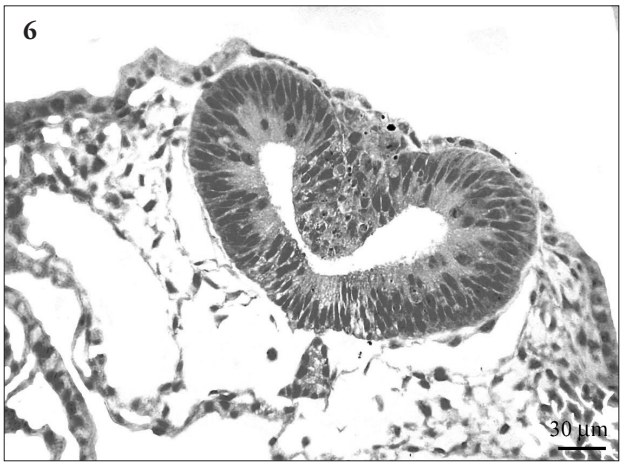

Fig. 6.- Exp-57 pih, H-E. The special form of the anomalous mesencephalon, along with the invasive neural crest cells, adopts the aspect of a playing card heart.

The Neural Crest. Exp: the cells were clearly visible (Figures 3-5). **GC**: unlike the Exp, the crest cells were difficult to visualise. **The Mesencephalon and Rhombencephalon. Exp:** The roof of the mesencephalon showed an indentation that became more pronounced later on, forming a groove. This groove was filled up with cells from the neural crest, forming a triangle between the mesencephalon and the ectoderm. These neural crest cells entered the mesencephalic lumen via the junction that previously joined both edges of the neural tube (Figure 3). After the layer of the roof cells of the mesencephalon had separated in the centre, they entered into the lumen, starting out as a group of a few cells. In the following section, made at 20-30 microns, the process had made so much progress that the cellular mass occupied 1/3 of the lumen of mesencephalon, and further on almost occupied the entire area, and the cellular invasion left only a thin circle of lumen around it. They formed an *isthmus* or peduncle and opened up like a bouquet to form the outer circle of the aforementioned cellular invasion. The neural cells stopped at the entrance of the isthmus (Figure 3). In the lumen of some of the sections, desquamated necrotic cells belonging to the cellular invasion, with picnotic nuclei, were seen. This cellular invasion extended from the beginning of the mesencephalon to the end of the rhombencephalon.

The neural cells of the mesencephalon were arranged in radial columns, with spaced out nuclei moving away from the lumen. However, on the floor and in the ventral-lateral area this was not the case; there was greater cellular density and the nuclei were more frequently located near the lumen. Furthermore, the lateral edges were slightly embossed (Figure 4). Frequently, the outermost cells of this lower area gave rise to a more or less indented edge and some cells displayed citoplasmatic areas, which were clearer. Sometimes, the lower tip of the playing card heart could not be seen, but just below this area and above the notochord there was a small ovoid cellular mass that could well represent this group of cells that had become detached from the mesencephalon (Figure 5). The floor of mesencephalon usually tapered into a point, which along with the aforementioned groove and the "bouquet" of invasive cells gave the mesencephalon the appearance of a playing card heart (Figures 4 and 6). **GC:** the following features were not present: a groove; cellular invasion in the lumen; lower edge indentation;

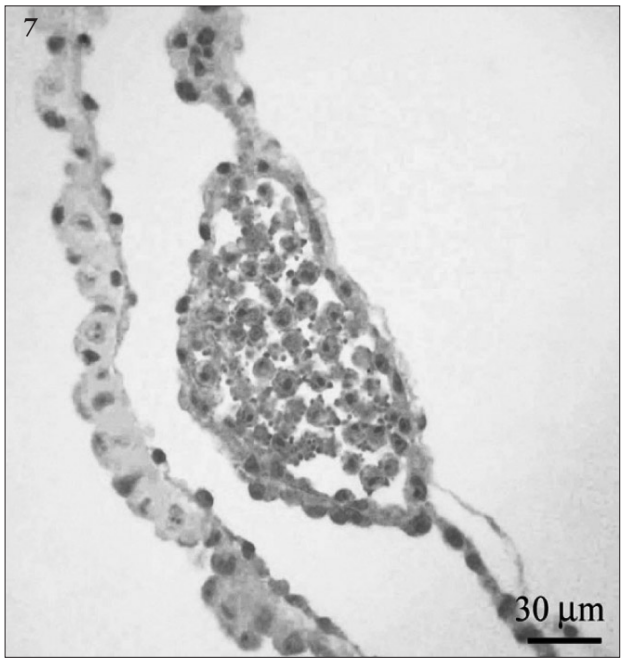

Fig. 7.- Exp-57 pih, H-E. Blood island in the splanchnopleure with papilliform or amoeboid primitive red blood cells, which is indicative of the delay of the development. This is evidence of cellular developmental delay.

slightly embossed lateral edges. **The Notochord. Exp:** this appeared as a vertical line of cells and the gut already existed. This shape is normal at the start (Bellairs and Osmond, 2005) but then changes further down the length of the notochord. Shortly after, it appeared as a triangular (and later ovoid) mass of cells. **GC:** this appeared with four cells, which increased to seven-eight cells further towards the caudad, and it remained circular.

Cutting Area C (10 serial sections)**. - Exp:** The ectoderm, the neural tube –this already displayed a vertical axis- the neural crest, the ovoid notochord and the gut, were all normal. The different blood vessels were in their proper position. All cardiac structures were seemingly normal. The somites were normal and split into derma-myotome and sclerotome. The mesoderm was still loosely arranged in comparison with the mesoderm of the GC. Two layers of cells (from the neural crest and the ectoderm) covered the roof of the neural tube. The somatopleure and splanchnopleure maintained the morphology of their cells. **IC:** a comparison of sections caudal to the anterior intestinal portal revealed that the somites had a better developed derma-myotome dorso-laterally, and that their sclerotome had a larger expansion area; the notochord had become considerably thicker, as had the neural tube; the start of the mesonephric tubules was visible in the IC but not in the Exp. These characteristics, among others, point to evident histological development delay between the Exp and the IC. **GC:** the notochord was somewhat circular, the mesoderm was compact, the neural tube was somewhat pear-shaped and the cardiac cavity had its epimyocardium and endothelium. The membranes of the somatopleure and the splanchnopleura had a normal thickness and stained well.

Cutting Area D (10 serial sections). **- The Somites. Exp:** papilliform cells in some somitocoeles were observed, which did not occur in GC. **The Neural Tube. Exp:** the neural plate was broken accidentally in the middle line, **GC:** the neural tube was still ovoid, with a straight and narrow lumen, surrounded by several hyaline cells layers of the ectoderm. **The Notochord. Exp:** this was normal. **The Somatopleure and Splanchnopleure. Exp:** in the blood islands there were papilliform primitive red blood cells in large quantities (see Figure 7: *Cutting Area E*). Bearing in mind that the first elements of the primary lineage are the large slightly amoeboid cells derived from blood islands (Romanoff, 1960) and that the first central cells of blood islands arise in embryos of 3 to 5 somites (around stage 8 HH) (Patten, 1952), it must be accepted that the development delay of the red series of the Exp blood is truly striking. **GC:** no papilliform primitive red blood cells were observed in their blood islands. We examined other control embryos that were younger (31-35.5 and 36.5 pih) and they all produced the same negative result.

Cutting Area E (5 serial sections). **- The Somatopleure and Splanchnopleure. Exp:** papilliform blood cells were observed in the splanchnic mesoderm (Figure 7). These characteristic cells were not observed in the GC.

Table 3. Developmental stage of the Exp-4 pid and its control embryos. Anatomical differences between the Exp-4 pid and its incubation control embryo, which had the same incubation time.

Embryo	Experimental	Incubation Control	Growth Control
Post incubation days	4 and 6 hours	4 and 6 hours	2 and 23 h
Stage according to pid	23-24 HH	23-24 HH	19 HH
Stage according to its growth	19 HH	23 HH	19 HH

ANATOMY	EXPERIMENTAL	INCUBATION CONTROL
Length of the embryo	1,7 cm	2.8 cm
The somites	37 pairs	43 pairs
The visceral arches	2nd, 3rd and 4th are visible (stage 21 HH)	1st- 4th are visible (stage 23 HH)
The limbs	Underdeveloped	Normally developed
The eye	Exterior opening of optic cup is wide	Here it is closing as the edges join together towards the lens
The ear	The same development	The same development
The nasal cavities	Larger	Normal
Torsion	Incomplete	Complete
Bending		
- The cranial flexure	Same	Same
- The cervical flexure	Less pronounced	Normal
- The trunk flexure	More marked	Normal
- The caudal flexure	Similar	Similar
The nervous system:		
- The *lamina terminalis*	Wider or more pronounced	Normal
- The telencephalic vesicles	Smaller	Normal
- The mesodiencephalic fold	Shallower	Normal
- The constriction of the *isthmus rhombencephali*	Shallower	Normal
- Volume of the mesencephalon	Markedly less developed	Normal
The epiphysis	Slightly underdeveloped	Normal
The liver	Considerably smaller	Normal
The heart		
- The apical area of ventricle is:	Rounder. Indicative of underdeveloped	Normal
Visceral mass of the trunk	Not very developed	Prominent

2a. COMPARATIVE ANATOMICAL STUDY OF THE 4 PID + 6 PIH **EXP** (19 HH) AND ITS 4 PID+ 6 PIH **IC** (23 HH)

The results are summarised in Table 3.

Comments: we used five IC, and obtained the average value for all the measurable values studied. Limbs: these will be described in another paper (Rodríguez-Burgos and Juárez, unpublished observations).

2b. COMPARATIVE HISTOLOGICAL STUDY OF THE 4 PID + 6 PIH **EXP** (19 HH) AND ITS 2 PID + 23 PIH) **GC** (19 HH)

Cutting Area A (38 serial sections). - No noteworthy histological differences were observed between the Exp and its corresponding GC in the following structures.

1) neural tube. 2) notochord. 3) mesencephalon. 4) internal carotid arteries. 5) anterior and posterior cardinal veins. 6) branch of the fifth cranial nerve. 7) coelom. 8) spinal ganglions (adjacent to the neural tube). 9) metencephalon. 10) pharyngeal arches, pharyngeal pouches and branchial grooves. 11) aortic arches. 12) mandible and maxillary branches of the fifth nerve. 13) fifth cranial ganglion. 14) oesophagus. 15) lung buds. 16) right and left atria. 17) *truncus arteriosus.* 18) *bulbus cordis.* 19) *sinus venosus*. 20) *ventriculum*. 21) auditory vesicles. 22) laryngeal-tracheal groove. 23) myelencephalon. 24) liver bud. 25) *ductus choledochus*. 26) Cuvier's duct. 27) *duodenum*. 28) pancreas. 29) lens. 30) optic cup. 31) retina and 32) pigment layer of the retina, lens vesicle, optic cup opening. 33) dorsal and ventral mesenteries. 34) wing bud. 35) dorsal aorta. 36) telencephalon. 37) diencephalon. 38) mesonephric ducts.

Cutting Area B (4 serial sections). - Histological differences were observed in the following structures: **The Ectoderm. Exp:** this was joined to the underlying somites, and had 1-2 layers of cells whereas the GC is made up of 2-3 layers of epithelial cells. **The Somites. Exp:** the myotome had empty and loosely arranged areas. The columnar epithelial tissue (Bellairs and Osmond, 2005) of the dermatome was very loosely arranged and it occasionally had interior cracks (Figure 8 and 10). **GC:** the dermatome had intercellular unions. The tissue was continuous, with hardly any intercellular spaces. There were no interior cracks. The typical 'cap shaped' structure, where the dermatome and the myotome had a continuous histological architecture, was perfectly visible (Figure 9 and 11). **The Mesenchyme. Exp:** the area of the mesenchyme that surrounded the mesencephalon, notochord and the gut, was markedly more loosely arranged (Figure 12) than the same tissue in the corresponding GC (Figure 13).

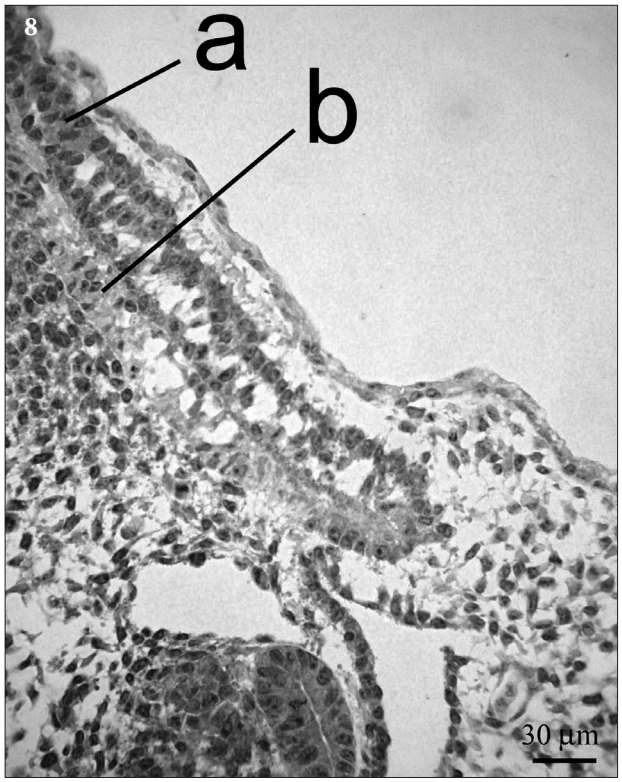

Fig. 8.- Exp-4 pid, H-E. (a) A dermatome with tissue disintegration. (b) A miotome shows empty areas.

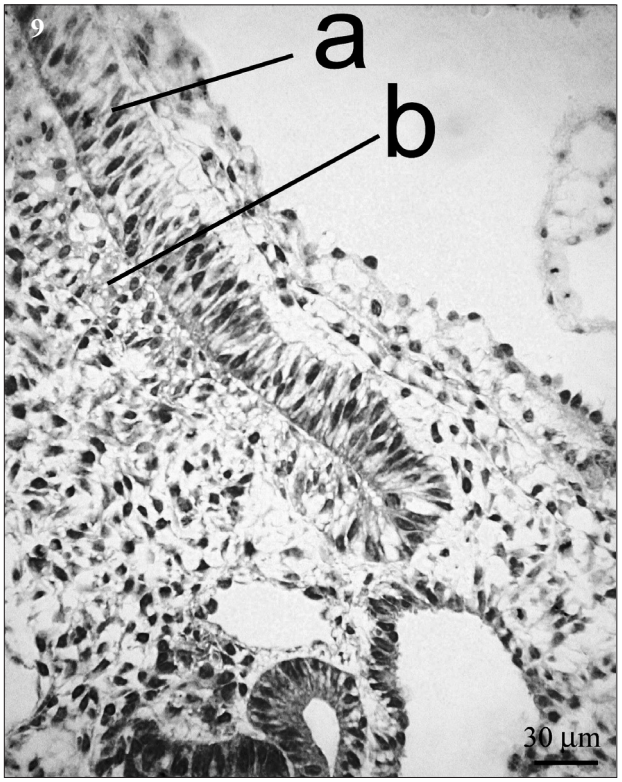

Fig. 9.- GC of the Exp-4 pid, H-E. (a) Dermatome and (b) myotome are normal.

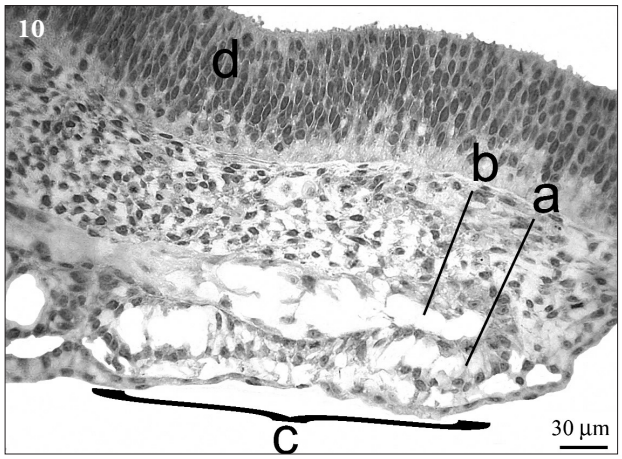

Fig. 10.- Exp-4 pid, H-E. (a) Dermatome and (b) myotome: widespread zones display cellular destruction (c) "Cap" structure almost conserved. (d) Myelencephalon. The mesenchyme is slightly less arranged than that of the GC (Fig. 11).

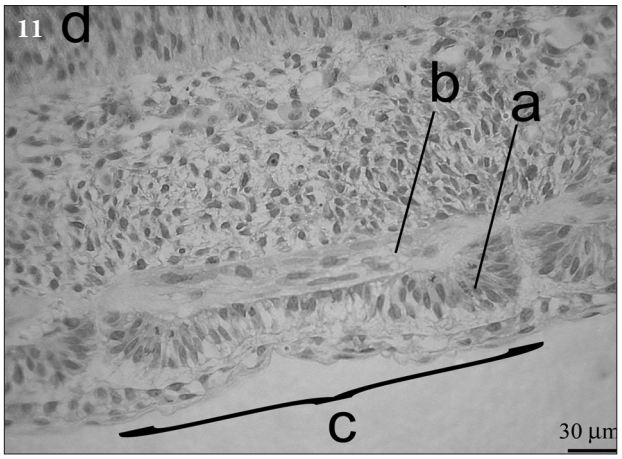

Fig. 11.- GC of the Exp-4 pid, H-E. (a) Dermatome and (b) myotome are normal (c) "Cap" structure perfectly conserved. (d) Myelencephalon. The mesenchyme is compact.

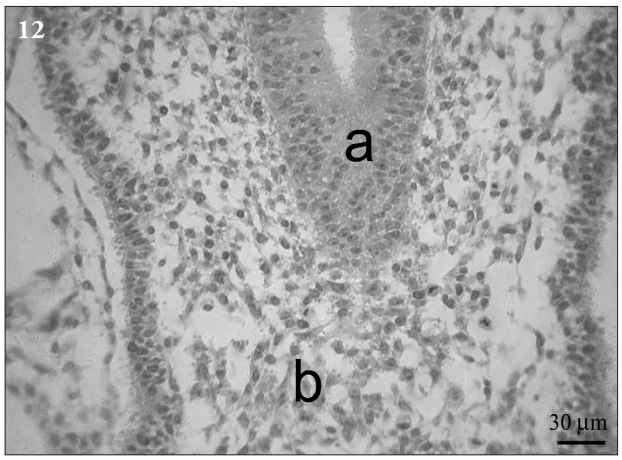

Fig. 12.- Exp-4 pid, H-E. (a) Gut. (b) Mesenchyme with loosely arranged cells.

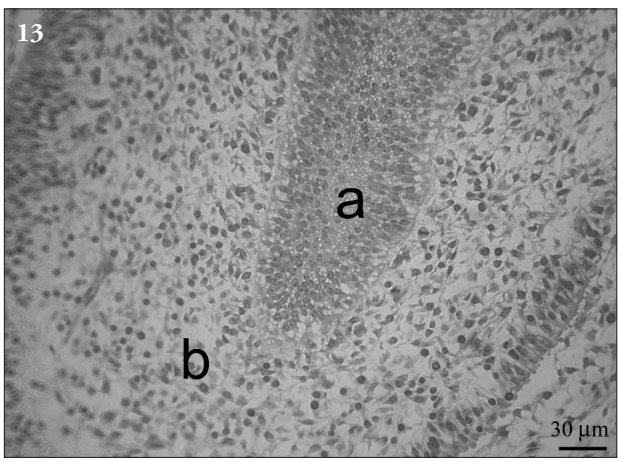

Fig. 13.- GC of the Exp-4, H-E. (a) Gut. (b) Mesenchyme with cells arranged compactly.

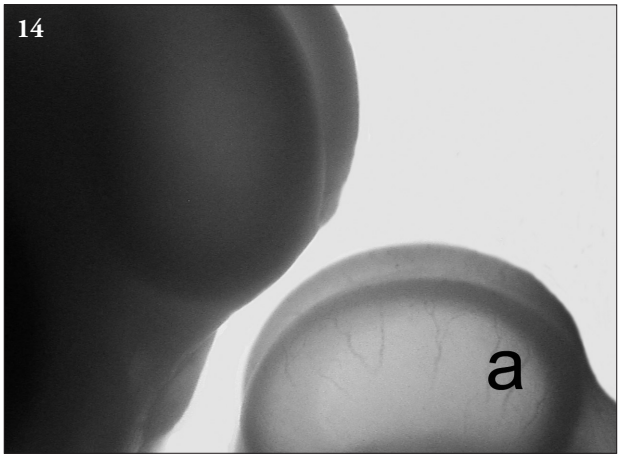

Fig. 14.- Exp-7 pid. Optic lobes in the mesencephalon. Left part: IC. Inferior right part: Exp-7 pid. (a) Tenuous vessels can be appreciated, which is indicative of retardation in development and growth. (see Table 3).

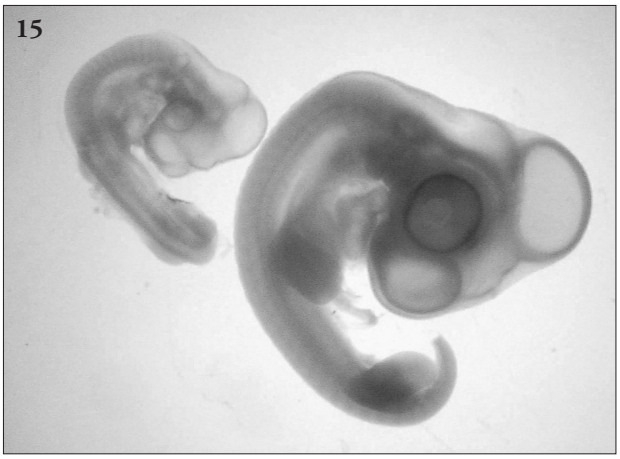

Fig. 15.- Size difference between Exp-4 pid (left) and its IC (right), both with the same time of incubation (4 days and 6 hours). This is a typical picture of gross anatomical growth retardation.

Cutting Area C (2 serial sections). - **The Allantois. Exp:** the following could be observed: a series of pseudocystic glomeruli, fewer blood vessels than in the GC, rounded tightly-bonded cells, with hardly any intercellular spaces. **GC:** there were very few intercellular spaces, and there were no pseudocystic glomeruli. **Join between the allantois and the cloacae. Exp:** pseudocystic glomeruli were still present. The cylindrical pseudostratified epithelium that covered the lumen had two layers in its ventral section. **GC:** there were no pseudocystic glomeruli, and the lumen epithelium had 3-4 layers in its ventral section. **Caudal End. Exp:** the mesoderm cells were more tightly bonded than in the GC, with no intercellular spaces (Bellairs and Osmond, 2005).

3a. COMPARATIVE ANATOMICAL STUDY OF THE 7 PID **EXP** (28 HH) AND ITS 7 PID **IC** (31 HH)

The results are summarised in Table 4.

Table 4.- Developmental stage of the Exp-7 pid and its control embryos. Anatomical differences between the Exp-7 pid and its incubation control embryo, which had the same incubation time.

EMBRYO	EXPERIMENTAL	INCUBATION CONTROL	GROWTH CONTROL
Post incubation days	7	7	6 + 4 pih
Stage according to pid	30-31 HH	30-31 HH	28 HH
Stage according to its growth	28 HH	31 HH	28 HH

ANATOMY	EXPERIMENTAL	INCUBATION CONTROL
Length: on cephalon-caudal axis	4.4 cm	4.9 cm
The limbs, HH	Underdeveloped	Normal
The visceral arches, K	Mandible process not yet fused with second pharyngeal arch. Neck has not begun to grow lengthwise Beak does not yet protrude from surface of the face	Fused Neck has increased in length Beak already protude
The nervous system HH, K, R - Notocord - Spine	Transitory blood vessels of optic lobes are visible, which is a characteristic of stage 28 HH (Fig. 14) It is flat and has a larger surface area Dorsal and ventral horns have not appeared in the grey matter	These blood vessels are not visible (Fig. 14) It is flatter and has normal surface area Dorsal and ventral horns are visible
The heart	Smaller in size	Normal
The mouth - The beak - The egg tooth - The mandible and the maxillary	 Smaller in size Not visible Protrude slightly from the surface of the face	 Normal Visible Normal
Gizzard	The circular muscular tissue barely exits	It has increased in size considerably. The circular muscular tissue barely exists, but it has already started to develop.
Thyroid gland or postbranchial bodies	The tissue does not yet have a saccular appearance	They have increased in size considerably, and the glandular epithelium now has a saccular or ribbed appearance
The lung buds	This has not yet occurred	There has been a diversification of the mesobronchi into secondary air sacs

ANATOMY	EXPERIMENTAL	INCUBATION CONTROL
The gut (caudal area)		
- The oesophagus	Its lumen is rounded	Its lumen has the shape of a cross
- The cloacae membrane	One fold, leaving a small hole (*proctadeum*)	Three folds
The eye		
- The iris	Not visible	Visible
- The choroid membrane	Not pigmented	Pigmented
- The eyelids	Lower eyelid	Circular fold (Upper and lower eyelid)
- The nictitating membrane	Not present	Beginning to develop
Bending		
- The cranial flexure	Angle is 45º	Almost the same
- The other flexures	Angle is 45º	Almost the same
The ear	Depression of long groove	Small shallow circular depression

Comments: Limbs: these will be described in another paper (Rodríguez Burgos and Juárez, unpublished observations). HH: Hamburger and Hamilton, 1951; K: Künzel, 1961; R: Romanoff, 1960.

3b. COMPARATIVE HISTOLOGICAL STUDY OF THE 7 PID **EXP** (28 HH) AND ITS 6 PID + 4 PIH **GC** (28 HH)

In the Exp we did not find anomalies with respect to its GC in the following structures:

Cutting Area A (32 serial sections). - 1) auditory vesicles. 2) myelencephalon. 3) metencephalon. 4) *isthmus*. 5) optic lobes and cerebral vesicles. 6) mesencephalon. 7) aqueduct of Sylvius. 8) retina. 9) choroid fissure. 10) lens. 11) metencephalon. 12) accessory nerve of the eleventh ganglion. 13) pineal gland. 14) diencephalon. 15) trigeminal ganglion. 16) semicircular ear canal. 17) hypophyseal anlage. 18) optic nerves. 19) jugular veins. 20) telencephalic vesicles. 21) dorsal root ganglion. 22) pharyngeal arches, pharyngeal pockets and branchial grooves. 23) nasal cavities. 24) carotid arteries. 25) pharynx. 27) tongue. 28) interorbital septum. 29) *corpus striatum*. 30) choroid plexus. 31) Monro's foramen. 32) parathyroid glands. 33) thymus. 34) trachea. 35) bronchial tubes. 36) omphalo-mesenteric arteries and veins. 37) Cuvier's ducts. 38) *sinus venosus*. 39) atria. 40) ventricles. 41) atrioventricular cushions. 42) interatrial, interventricular and aortic-pulmonary septa. 43) arterial trunk. 44) dorsal aorta. 45) pulmonary arteries. 46 cardinal veins. 47) liver. 48) neural arch. 49) vertebra buds. 50) dorsal and ventral mesenteries. 51) mesonephros. 52) crop. 53) proventricle.

Cutting Area B (10 serial sections). - 1) hepatic artery and vein. 2) dorsal aorta. 3) dorsal mesentery. 4) mesonephros. 5) pancreas. 6) *ductus choledochus.* 7) biliary vesicle. 8) spleen. 9) subcardinal veins. 10) rotation of the intestine. 11) gonads 12) celiac artery. 13) duodenum, jejunum and ileum. 14) caecum. 15) oviducts. 16) colon and rectum. 17) cloacae. 18) bursa of Fabricius. 19) renal arteries. 20) allantoic stalk. 21) allantoic artery and vein. 22) metanephric ducts.

DISCUSSION

There is extensive literature that deals with the subject of foetal growth retardation owing to the importance that this syndrome has for health during adult life (Barker et al., 1993; Osmond and Barker, 2000; Barker et al., 2002). Foetal undernourishment seems to be its best defined cause (Mahajan et al., 2004). Vaillancourt and McCallion (1972) demonstrated that the antibodies of nephrotoxic antisera blocked the nutritional function of the yolk sac and produced foetal GR in the rat embryo. At the current stage of our investigations, we cannot affirm whether some sFF-Ag might carry out the same function at the level of the yolk sac or whether it acts in a different way. In contrast, we have elsewhere reported that GR take place in a large number of embryos (Rodríguez Burgos and Juárez, unpublished observations), from among which we chose the three studied here (Figure 15). Nevertheless, we emphasise the developmental delay that we detected in many of the organs and anatomical structures, as we indicated in Tables 1, 3 and 4, which for us suggests that the decrease of the size and the weight of the embryo, which characterises this syndrome, also implies the existence of an immaturity or delay in its development. This occurs at histological level (e.g. heart) and at a cellular level (e.g. papilliform red cells), both in the Exp-57 pih.

With the exception of generic reactions such as monstrosity, foetal death, and GR, in

none of our 60 abnormal embryos (Rodríguez-Burgos, 2003; Rodríguez-Burgos and Juárez, unpublished observations) did we observe the alterations described by authors who used the conventional method to administer heterologous antibodies to the embryo against antigens of the adult chicken, the differentiation antigens, or the ample mixture of antigens contained in the embryo extract. This is perhaps because in our case the embryos only received isologous antibodies, anti-sF-TrAg and anti-sAlloAg, from their dams. Therefore, our results cannot be compared with those of the above authors, nor even with those of the few authors who made a reduced histological study from altered tissues (Langman et al., 1962; McCallion, 1971; among others).

We shall now focus on the most striking histological alterations of the embryos studied and we shall address their possible relationship with congenital anomalies observed in the chickens born alive in this same experiment (Rodriguez-Burgos, 2003; Rodríguez-Burgos et al., unpublished observations).

In the Exp-57 pih there was an invasion of neural crest cells in the lumen of the neural tube, which was present right from the start of the mesencephalon to the end of the rhombencephalon, and not before nor after. Since we knew that three poults were born with transitory ataxia and difficulties in pecking food and drinking, it seemed reasonable to argue that these poults had undergone those alterations, but to a minimal degree, so that they were viable (Rodríguez-Burgos et al., unpublished observations). There was a strikingly abnormal development of the *infundibulum* in the thickness itself of the ventral prosencephalon. This fuses with Rathke's pocket to give rise to the pituitary. Given the dramatic alteration in the *infundibulum* and the vital role played by the pituitary, it was not surprising that this anomaly should produce non-viable chick embryos. However, the possibility also exists that if this alteration occurs to a lesser degree in other embryos, they may well be born, but would have congenital endocrine disorders. In the chicks that were born in this experiment this possibility did not arise (Rodríguez-Burgos, 2003; Rodríguez Burgos et al., unpublished observations). The last specific alterations involved the loose arrangement of the mesenchymal tissue (see below) and the presence of papilliform blood island cells, as a cellular expression of developmental delay, and of papilliform cells inside some somites.

The Exp-4 pid displayed an alteration in the structure of the somites (dermatomes and myotomes), and a loose arrangement in certain areas of the mesenchymal tissue. We cannot rule out that the alterations in the dermatome and myotome could be a consequence of the apoptotic activity present in embryonic development. Nevertheless, this interpretation must be treated with caution since these histological alterations were not found in the controls. The loose arrangement of the mesenchymal tissue, seen in the Exp-57 pih and Exp-4 pid, the alterations in the myotomes, in the Exp-4 pid, should be linked to the congenital scoliosis that one of the aforementioned poults displayed as an adult (Rodríguez-Burgos et al., unpublished observations). The mesenchymal tissue gives rise to the connective tissue, which plays such an important role in the structure of the spine and its ligaments. These data should be borne in mind in future studies on the pathogenesis of scoliosis, given that a fair number of authors have attributed the origin of this disorder to a failure in connective tissue. We should also mention the alterations observed in the myotomes, since their cells give rise to the paravertebral musculature, among other structures. Similarly, other authors have linked a deficiency in this musculature to the genesis of scoliosis.

In the Exp-7 pid we observed a delay in growth throughout the body, although this delay was slightly more pronounced in certain organs, e.g. the pharyngeal arches, the neck, the limbs and the beak. Furthermore, no developmental anomalies were detected at histological level.

We considered it useful to publish these pioneering results, given their high histological specificity and given the novelty of the antigens involved. We hope the current research will justify and guide later studies. In our opinion, the best experimental design is to purify each of the sFF-Ag and immunise different batches of hens with each of them (Rodríguez-Burgos, 2004). It will then be possible to carry out studies with varied and specific stains, statistical data, electron microscopy images, immunohistochemistry, etc. We believe that by doing this, most of the enigmas present in this research will disappear, although perhaps new ones will also arise.

Acknowledgements

We would like to thank Professor R. Bellairs (Department of Anatomy and Developmental Biology, University College London) for reading the manuscript and offering crucial suggestions. We also thank Professor R. Vaamonde, Chairman of the Department of Histology, whom very kindly carried out the morphometric study, and Professor J. Aceitero, Department of Anatomy, with whom we had fruitful discussions (Faculty of Medicine, University of Cordoba). We also thank Dr. J. Salas, Service of Pathology of the Hospital Reina Sofía (Córdoba) for his help in the histological work.

References

Barker DJ, Hales CN, Fall CH, Osmond C, Phipps K and Clark PM (1993). Type 2 (non-insulin-dependent) diabetes mellitus, hypertension and hyperlipidaemia (syndrome X): relation to reduced fetal growth). *Diabetologia,* 36: 62-67.

Barker DJ, Eriksson JG, Forsen T and Osmond C (2002). Fetal origins of adult disease: strength of effects and biological basis. *Int J Epidemiol*, 31: 1235-1239.

Bellairs R and Osmond M (2005). Atlas of Chick Development. 2nd ed. Elsevier, London.

Clarke WM and Fowler I (1961). The inhibition in lens-inducing capacity of the optic vesicle with adult lens antiserum. *Proc Soc Exp Biol Med,* 106: 155-172.

García del Moral R (1955). Laboratorio de Anatomía Patológica. Interamericana-McGraw-Hill, Madrid.

Genís-Gálvez JM, Castro JM de and Battaner E (1967). Effect des antiserums anti-cristallin sur la différenciation morphologique du cristallin chez l'embryon de poulet. Bull Ass Anatomistes 52e Réunion, 559-564. Paris-Orsay, 2-6 Avril.

Hamburger V and Hamilton HL (1951). A series of normal stages in the development of the chick embryo. *J Morphol,* 88: 49-92. (Reprinted *Develop Dynamics,* 195: 231-272).

Künzel E (1961). Die Entwicklung des Hühnchens im Ei. *Zbl Vet Med,* 9: 371-395.

Langman J, Maisel H and Squires J (1962). The influence of lens antibodies on the development of lens antigen-containing tissues in the chick embryo. *J Embryol Exp Morph,* 10: 178-190.

Mahajan SD, Singh S, Shah P, Gupta N and Kochupillai N (2004). Effect of maternal malnutrition and anemia on the endocrine regulation of fetal growth. *Endocr Res,* 30: 189-203.

McCallion DJ (1971). Teratogenic effects of tissue-specific antibodies in the chick embryo. *Biol Neonate,* 18: 153-159.

Mun AM (1958). Toxic effects of normal sera and homologous antisera on the chick embryo. *Biol Bull,* 15: 239-256.

Osmond C and Barker DJ (2000). Fetal, infant, and childhood growth are predictors of coronary heart disease, diabetes, and hypertension in adult men and women. *Environ Health Perspec,* 108 Suppl 3: 545-553.

Rodríguez-Burgos A (2003). Detection in chick embryo of fetoproteins not recognized by the dam's immune system and of soluble alloantigens. Teratogenic and abortogenic capacity of their specific IgY. *BMC Immunology,* 4, 6.
http://www.biomedcentral.com/1471-2172/4/6.

Rodríguez-Burgos A (2004). New fetoproteins, as presumptive antigenic inducers of abortions and congenital anomalies. Temporal forking of immunological abortions. A working hypothesis. *Medical Hypotheses,* 63: 47-55.

Rodríguez-Burgos A and Juárez L (unpublished observations). Developmental delay, intraovo growth retardation, and embryonic and perinatal death in the offspring from hens immunized to chick embryo soluble and foreign antigens (in preparation).

Rodríguez-Burgos A, Juárez L, Miró F, Vázquez F, Ocaña JM and Novales M (unpublished observations). Congenital birth defects in poults from hens immunized to chick embryo soluble and foreign antigens (in preparation).

Romanoff AL (1960). The Avian Embryo: Structural and Functional Development. The Macmillan Co, New York.

Sánchez Palazón L, Copado MA, Ruiz-Gutiérrez V and Rodríguez-Burgos A (1996). Antibodies to alpha-fetoprotein disrupt histogenesis in cultured chick retinae. *Tissue Cell*, 28: 223-226.

Smith JA (1973). Effect of antibody to α-fetoprotein in the development of chicken and rat embryos. *Archiv Immunol Therap*, 21: 163-173.

Vaillancourt P and Mccallion DJ (1972). Inhibitory effects of nephrotoxic antisera on the growth of rat fetuses. *Am J Obstet Gynecol,* 114: 255-258.